ACS OMEGA

http://pubs.acs.org/journal/acsodf

Article

Accelerating ^{1}H NMR Detection of Aqueous Ammonia

Martin Kolen,* Wilson A. Smith, and Fokko M. Mulder*

Cite This: *ACS Omega* 2021, 6, 5698−5704

Read Online

ACCESS | Metrics & More | Article Recommendations | Supporting Information

ABSTRACT: Direct electrolytic N_2 reduction to ammonia (NH_3) is a renewable alternative to the Haber−Bosch process. The activity and selectivity of electrocatalysts are evaluated by measuring the amount of NH_3 in the electrolyte. Quantitative ^{1}H nuclear magnetic resonance (qNMR) detection reduces the bench time to analyze samples of NH_3 (present in the assay as NH_4^+) compared to conventional spectrophotometric methods. However, many groups do not have access to an NMR spectrometer with sufficiently high sensitivity. We report that by adding 1 mM paramagnetic Gd^{3+} ions to the NMR sample, the required analysis time can be reduced by an order of magnitude such that fast NH_4^+ detection becomes accessible with a standard NMR spectrometer. Accurate, internally calibrated quantification is possible over a wide pH range.

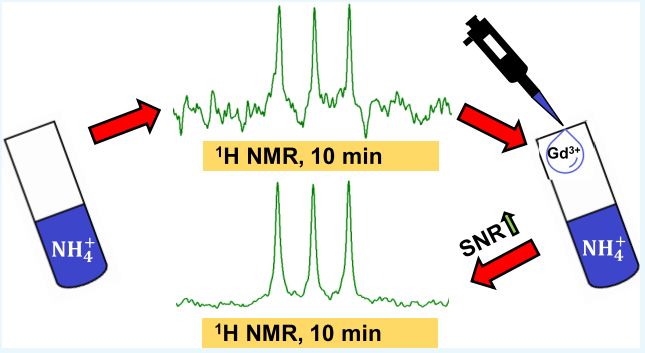

INTRODUCTION

Ammonia (NH_3) is one of the largest chemical commodities responsible for about 1.5% of global energy use and associated CO_2 emissions from the Haber−Bosch process. Its primary use is as a feedstock for nitrogen-based fertilizers. Electrochemical, fossil-fuel-free methods to produce ammonia are gaining significant interest for the reduction of CO_2 emissions, as well as enable ammonia as a carbon-free energy carrier and storage material.[1−3] Direct electrolytic N_2 reduction is a renewable alternative to synthesize NH_3. To suppress the undesirable hydrogen evolution reaction, a selective electrocatalyst is needed.[4]

The activity and selectivity of electrocatalysts are quantified by measuring the accumulated NH_3 in the electrolyte with appropriate detection methods. Recently, a number of papers were published concerning the difficulty of obtaining reproducible results in nitrogen reduction research.[5,6] Such difficulty is related to experimental procedures and significant amounts of NH_3 from dust, ambient air, $^{15}N_2$, and desorption from cell surfaces. In addition, NOx contamination or nitrogen-containing catalyst precursors can be reduced to NH_3 during electrolysis, which can be falsely attributed to N_2 reduction.[7,8] Reliable testing and analysis procedures including control experiments with an isotope labeled $^{15}N_2$ are necessary to avoid false positives.[5] Conventional spectrophotometric NH_3 detection methods such as the indophenol blue method cannot distinguish between isotopologues of NH_3 and require considerable bench time.[9,10] ^{1}H NMR spectroscopy is a fast, accessible, and isotopically selective alternative to spectrophotometric methods for NH_3 detection, but as we will show below, the sensitivity on a standard 400 MHz spectrometer is insufficient.[11] Here, we present a powerful liquid-state NMR method with sufficient sensitivity on relatively easily accessible NMR spectrometers, i.e., requiring limited field strength and normal sensitivity probes.

Several alternatives to spectrophotometric NH_3 detection methods have been proposed recently. Ion chromatography can be used for ammonia detection but isotopologues cannot be distinguished and an overlap of NH_4^+ with other cations poses a threat to the accuracy of the method.[12] Yu et al. proposed ultrahigh-performance liquid chromatography−mass spectroscopy (UPLC-MS) to measure derivatized solutions of NH_3.[13] The method is very sensitive and capable of distinguishing isotopologues of NH_3 but requires careful control over the pH. Quantitative ^{1}H NMR has been widely adopted to quantify $^{15}NH_4^+$ from control experiments with $^{15}N_2$. The acidified form of ammonia, ammonium ($^{14}NH_4^+$), and its isotopologue $^{15}NH_4^+$ have an unmistakable fingerprint in the ^{1}H NMR spectrum.[11]

Quantitative ^{1}H NMR is based on the proportional relationship between the signal integral I_x and the number of protons N_x responsible for that particular signal

$$I_x = K_S N_x \quad (1)$$

Received: December 16, 2020
Accepted: February 9, 2021
Published: February 19, 2021

https://dx.doi.org/10.1021/acsomega.0c06130
ACS Omega 2021, 6, 5698−5704

where K_S is a proportionality factor that depends on the physicochemical properties of the sample. To achieve accurate quantification, changes in K_S have to be accounted for by a suitable quantification method.[14] Pulse length-based concentration determination (PULCON) uses the principle of reciprocity to correlate the absolute intensity of two spectra measured in different solutions.[15] Nielander et al. successfully applied the PULCON method to NH_4^+ quantification.[11]

Since fluctuations of K_S affect all resonances in the spectrum equally, the ratio of two peaks is independent of K_S and can therefore be used for quantification. Typically, an internal standard of known concentration is added as a reference. The concentration of NH_4^+ can be quantified by either relative or absolute quantification. For relative quantification, a calibration curve is generated by measuring standard solutions of NH_4^+ and an internal standard.[14] The prerequisites for accurate ammonia quantification with relative quantification were recently described..[16] Absolute quantification allows the calculation of the NH_4^+ concentration directly from the integral of the peaks of NH_4^+ and the internal standard without requiring a calibration curve according to

$$C_{NH_4^+} = \frac{I_{NH_4^+}}{I_{std}} \frac{N_{std}}{N_{NH_4^+}} C_{std} \quad (2)$$

where I, N, and C are the integral area, number of nuclei, and concentration of NH_4^+ and standard, respectively. Absolute quantification requires that the total time spent to acquire one scan, the interscan delay t_{scan}, is at least 5 times the longest longitudinal relaxation time T_1 in the sample.[14] Despite the advantages of absolute quantification (calibration-free and robust) so far, no absolute quantification method has been proposed for ammonia detection. Hodgetts et al. reported that a d_1, T_1, and proton exchange-induced loss of coherence affects the NH_4^+ peak, rendering absolute quantification not suitable for NH_4^+ detection.[16] By adding a suitable paramagnetic salt, accurate absolute quantification becomes possible because the T_1 values of both the internal standard and NH_4^+ are reduced so that there is insufficient time for the proton exchange to induce a loss of coherence as we will see below.

The lower limit of quantification (LOQ) of a detection method is the lowest concentration of NH_3 that can be measured within an acceptable time and with an acceptable accuracy. The LOQ depends on the sensitivity, which is calculated from the signal-to-noise ratio (SNR) at a certain interscan delay t_{scan}

$$\text{sensitivity} = \frac{\text{SNR}}{t_{scan}} \quad (3)$$

To reduce the minimum LOQ by a factor of 2, the analysis time has to be quadrupled.[17] Nielander et al. could detect 1 μM NH_4^+ in ethanol within 1 h (t_{scan} = 2 s) with a 900 MHz NMR and cryo-probe.[11] The sensitivity difference between a 900 MHz NMR and a standard laboratory NMR (400 MHz) is substantial. The type of probe and the field strength difference lead to 1 order of magnitude lower sensitivity, which leads to 2 orders of magnitude longer analysis time to achieve the same LOQ on a 400 MHz NMR without cryo-probe.[18] To compensate for the lower sensitivity, longer experiments (typically several hours) are necessary to accumulate enough NH_4^+ in the electrolyte to reach the detection limit, which is unfavorable and which in addition increases the risk of false negatives due to deactivation and of false positives due to contamination. Higher ^{1}H NMR sensitivity is needed to enable laboratories with more standard NMR spectrometers to quantify NH_3 efficiently.

The type of the pulse sequence influences the NH_4^+ sensitivity strongly.[11,16] The signal from the hydrogen atoms of the solvent has to be suppressed to avoid baseline distortions and low receiver gain. Nielander et al. showed that pulse sequences that utilize pulsed field gradients in combination with selective excitation pulses are very effective at suppressing water without removing the NH_4^+ signal.[11] These pulse sequences use pulsed field gradients to dephase the water resonance and selective pulses to ensure that during acquisition water is completely out of phase while NH_4^+ is in phase.[19]

The T_1 of a molecule influences the sensitivity, because for a given interscan delay t_{scan}, T_1 determines the percentage of spins that can relax back to equilibrium in between scans. A smaller percentage relaxation leads to less acquired signal per scan according to

$$M_z = M_0(1 - e^{-t_{scan}/T_1}) \quad (4)$$

where M_z and M_0 are the magnetization in the z-axis following t_{scan} and at full relaxation, respectively. The interscan delay t_{scan} is composed of the recycle delay d_1 and the acquisition time. It is noteworthy that for some pulse sequences, the percentage relaxation only depends on the recycle delay, not on the acquisition time, as will be discussed in more detail below. Reducing the interscan delay, for example, by fast sampling is a well-known strategy to improve the ^{1}H NMR sensitivity.[20] Another strategy to lower the interscan delay is to shorten the T_1 of the analyte, which has the advantage that the same percentage relaxation can be achieved at a lower interscan delay.[14] T_1 is determined by the fluctuating magnetic interactions due to nearby magnetic moment fluctuations and due to positional changes of surrounding nuclei and moments. Interactions with unpaired electrons of paramagnetic substances are 1000 times larger than typical interactions between nuclear magnetic moments. Therefore, a small amount of a paramagnetic substance is sufficient to lower T_1 drastically.[21] This concept is applied in contrast agents for medical magnetic resonance imaging (MRI). The so-called paramagnetic relaxation enhancement (PRE) is also a common strategy to overcome sensitivity barriers for small organic molecules and proteins, because as T_1 decreases, more scans can be acquired in the same amount of time.[18,22,23]

RESULTS AND DISCUSSION

The Gd^{3+} ion is widely used for PRE in medical MRI due to its large magnetic moment from seven unpaired electrons.[24] We investigated the influence of paramagnetic Gd^{3+} ions on the sensitivity for aqueous ammonia detection to enable ^{1}H NMR as a routine analysis tool for NH_4^+ quantification, with the use of an internal standard (absolute quantification). In agreement with Nielander et al., we found that pulse sequences that are suppressing the water resonance by dephasing it during acquisition are well suited for NH_4^+ detection.[11] With excitation sculpting (ES), the water resonance is suppressed effectively and a flat baseline is obtained around the NH_4^+ triplet. However, at 40 μM NH_4^+, the SNR is only 13.6 for a 12.8 min measurement on a 400 MHz NMR with room-temperature probe (see Figure 1a). With this sensitivity, it takes 4 h until the accumulated ammonia in the electrolyte

https://dx.doi.org/10.1021/acsomega.0c06130
ACS Omega 2021, 6, 5698−5704

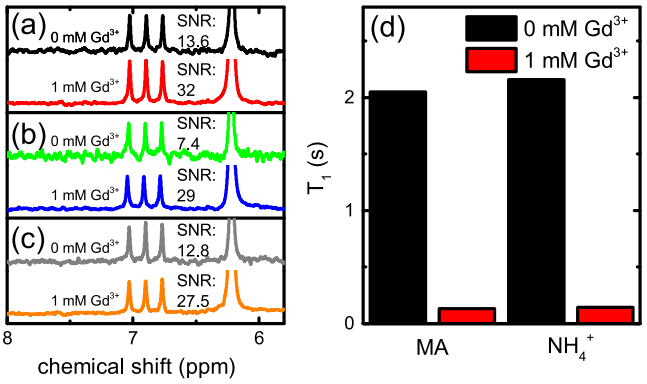

Figure 1. ^{1}H NMR sensitivity gain from 0 mM Gd^{3+} (black, green, and gray) to 1 mM Gd^{3+} (red, blue, orange) in the NMR tube measured with different acquisition parameters and pulse sequences. (a) 40 μM NH_4^+ measured with identical total acquisition time (12.8 min) and a recycle delay d_1 of 10 and 0.75 s for 0 mM Gd^{3+} and 1 mM Gd^{3+}, respectively. Pulse sequence: Excitation sculpting. (b) 40 μM NH_4^+ measured with identical total acquisition time (10.7 min) and recycle delay (0.5 s). Pulse sequence: Excitation sculpting. (c) 40 μM NH_4^+ measured with the same acquisition parameters as (b) but with the double pulsed field gradient spin echo (DPFGSE) pulse sequence. All SNR values are averages from a triplet measurement. (d) Effect of 1 mM Gd^{3+} on T_1 of NH_4^+ and maleic acid. Field strength: 400 MHz.

produced by a catalyst with intermediate activity becomes quantifiable by NMR (calculation in the Supporting Information, SI). Therefore, we sought to improve the sensitivity by adding 1 mM paramagnetic Gd^{3+} to the NMR tube. Maleic acid (MA) was added as an internal standard to quantify the amount of NH_4^+ with absolute quantification. The singlet of maleic acid at ca. 6.21 ppm is sufficiently separated from the NH_4^+ triplet at ca. 6.9 ppm. The T_1 values of both NH_4^+ and MA decrease drastically after the addition of Gd^{3+}. T_1 decreases from 2.16 to 0.14 s and from 2.05 to 0.13 s for NH_4^+ and MA, respectively. This 15.4-fold reduction of the T_1 of NH_4^+ enables a reduction of the interscan delay by the same factor, which, according to eq 3, leads to a potential 3.9-fold sensitivity increase ($\sqrt{15.4} = 3.9$). The linewidth of NH_4^+ increases only slightly with the addition of Gd^{3+} from 3.6 to 4.2 Hz.

To show that the measured sensitivity gain matches the sensitivity gain predicted from T_1 measurements, we measured a sample of 40 μM NH_4^+ with and without 1 mM Gd^{3+} using different acquisition parameters (Figure 1a–c). In Figure 1a, the total analysis time is identical in both measurements and d_1 is set to $5T_1$ so that NH_4^+ has the same percentage relaxation in both cases. With 1 mM Gd^{3+}, the sensitivity is significantly (factor 2.4) higher but not as much as expected from the T_1 decrease (factor 3.9). We will later show that a sensitivity gain close to the predicted value can be measured directly by removing an additional 90° pulse that is by default included in the ES pulse sequence. With the default version of ES, the sensitivity gain is lower than expected from the T_1 decrease because the additional 90° pulse removes the contribution of the acquisition time to the percentage relaxation. Consequently, the acquisition time only adds time to the total analysis time without improving signal strength and the percentage relaxation depends only on d_1. Since the acquisition time makes up a larger fraction of the interscan delay at low interscan delays, the decrease of sensitivity is more pronounced with 1 mM Gd^{3+} where the acquisition time makes up 0.75 s of the total 1.5 s interscan delay. Without Gd^{3+}, only 2 s out of 12 s interscan delay is the acquisition time that leads to a smaller sensitivity loss. In other words, the interscan delay could be factors 1.2 and 2 smaller for 0 mM Gd^{3+} and 1 mM Gd^{3+}, respectively. Therefore, the sensitivity gain with 1 mM Gd^{3+} would increase by a factor 1.3 ($\sqrt{\frac{2}{1.2}} = 1.3$) from 2.4 to 3.1 if the sensitivity loss would have been equal in both cases. Taking into account ≈15% sensitivity loss due to line broadening, the sensitivity gain is 3.6, which is close to the predicted value.

The experiment shown in Figure 1a is not sufficient to prove a sensitivity gain because it only shows that with a higher recycle delay, less scans can be acquired in the same amount of time. Less scans will always lead to lower SNR. To prove a sensitivity increase, it is necessary to show that a larger recycle delay is necessary with 0 mM Gd^{3+} but not with 1 mM Gd^{3+}. This is shown in Figure 1b, where both 0 mM Gd^{3+} and 1 mM Gd^{3+} were measured with low recycle delay (0.5 s) and identical total acquisition time. The sensitivity without Gd^{3+} is 3.9 times lower, indicating that a large fraction of the signal is lost due to low percentage relaxation. The percentage relaxation at a recycle delay of 0.5 s is 20.7 and 97.2% for T_1 of 2.16 and 0.14 s, respectively. Therefore, 4.7 times more signal can be expected with 1 mM Gd^{3+} in the same amount of time. We assume that 15% of that signal increase is lost due to line broadening with Gd^{3+}, which results in sensitivity improvement by a factor of 4.08. This value agrees well with the experimentally observed value of 3.9.

To study if adding Gd^{3+} also improves the sensitivity with other pulse sequences, we measured the sensitivity gain with the double pulsed field gradient spin echo (DPFGSE) pulse sequence (Figure 1c) using the same acquisition parameters as in Figure 1b. The sensitivity gain with DPFGSE (2.1) is lower than with ES (3.9). The reason for this is that with DPFGSE, the percentage relaxation has to be calculated using the full interscan delay including acquisition time, not just the d_1 as for ES. Using the same methodology as in (b), we calculate the percentage relaxation with and without Gd^{3+} and arrive at an expected sensitivity gain of 1.8, which agrees well with the experimentally measured value. The sensitivity gain is lower than in (b) because with 1 mM Gd^{3+}, the chosen t_{scan} of 1.25 s is almost 9 times longer than the T_1 of NH_4^+, which means that t_{scan} is much longer than the necessary $5T_1$, and as a result, sensitivity is lost. The previous examples demonstrate that after addition of 1 mM Gd^{3+}, a significant sensitivity gain is observed with different acquisition parameters and pulse sequences, and this sensitivity gain agrees well with the expected values predicted from T_1 measurements.

We measured the accuracy of NH_4^+ quantification with 1 mM Gd^{3+} by calculating the NH_4^+ concentration from the intensities of MA and NH_4^+ using eq 2 and comparing it to the gravimetrically measured concentration (Figure 2a,b). The method has very good linearity ($R^2 = 0.999$) and an acceptable relative error (≤10%) in the NH_4^+ concentration range of 30–388 μM with the ES pulse sequence. The relative error is randomly distributed around the abscissa, which suggests that it is caused by integration errors. Higher accuracy (relative error ≤ 5.3%) was obtained with an isotope labeled $^{15}NH_4^+$ (see Figure S2). $^{15}NH_4^+$ can be quantified with higher accuracy because it appears in the NMR spectrum as a doublet, which has inherently higher SNR than the $^{14}NH_4^+$ triplet.

https://dx.doi.org/10.1021/acsomega.0c06130
ACS Omega 2021, 6, 5698–5704

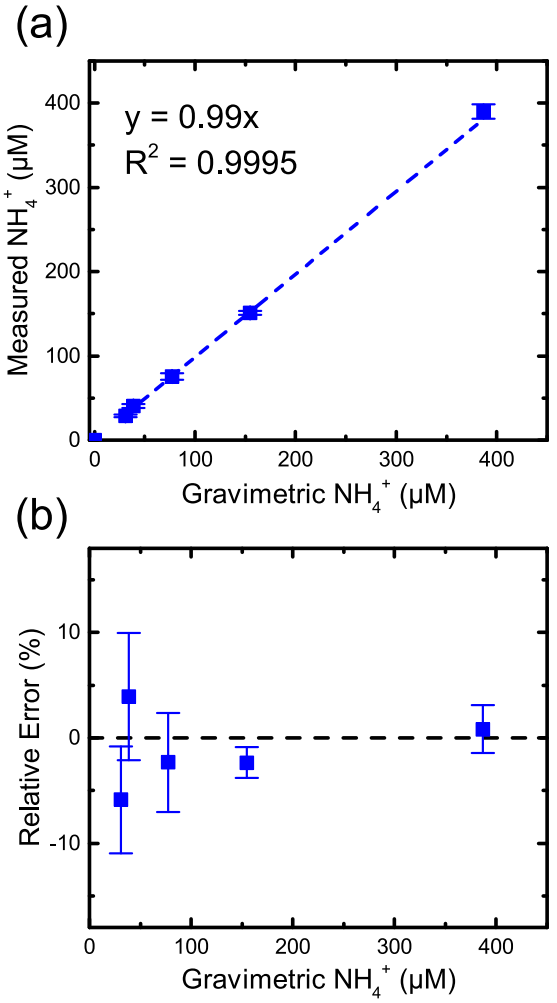

Figure 2. (a) Linearity and (b) accuracy of NH_4^+ quantification with 1 mM Gd^{3+}. Error bars around each point represent the standard deviation for each triplicate measurement. Pulse sequence: Excitation sculpting, recycle delay: 0.5 s, acquisition time: 0.75 s, total analysis time: 10.7 min, field strength: 400 MHz.

The pH of the catholyte, which is used for detection, can vary over time due to acidic or alkaline species produced in the electrochemical reaction or because of migration of ions induced by the electric field.[25,26] N_2 reduction experiments are especially prone to pH changes because the electrolyte volume is minimized to maximize the signal for ammonia detection. Both UPLC-MS and the indophenol method are sensitive to pH changes because the pH influences the reaction that is carried out prior to analysis.[9,13] Therefore, additional dilution steps can be necessary to measure accurately with these methods.

To investigate if the accuracy of our ^1H NMR method depends on the pH, we acidified a sample of 388 μM NH_3 with different concentrations of H_2SO_4 (Figure 3a). Based on the previous finding that the T_1 values of NH_4^+ and MA are very close to each other, we chose a recycle delay of 0.5 s ($3T_1$) for this experiment. For acid concentrations above 37 mM H_2SO_4, the relative error continuously increases when more acid is added. To investigate if the growing relative error might be caused by changing T_1 values, we measured the T_1 values of NH_4^+ and MA at 370 mM H_2SO_4 (Figure 3b). The gap between the T_1 values of NH_4^+ and MA is slightly larger at 370

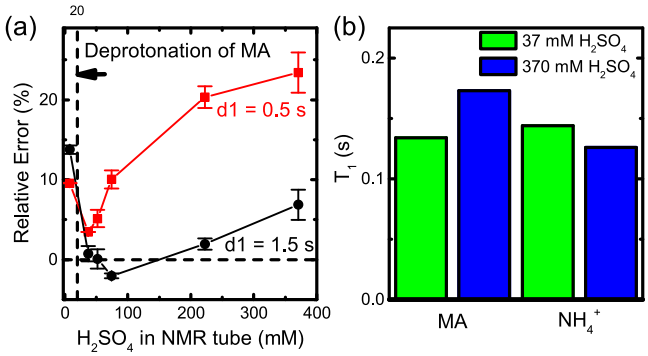

Figure 3. Influence of H_2SO_4 concentration in the NMR tube on the accuracy of NH_4^+ quantification with d_1 of 0.5 s (red) and 1.5 s (black). Error bars around each point represent the standard deviation for each triplicate measurement. (a) T_1 of NH_4^+ and maleic acid at two different H_2SO_4 concentrations. (b) Acquisition parameters: at = 0.75 s, nt = 512, Pulse sequence: Excitation sculpting, field strength: 400 MHz.

mM H_2SO_4 than at 37 mM H_2SO_4 which might explain the larger error. After increasing the recycle delay from 0.5 to 1.5 s to compensate for the increased T_1 gap, the relative error decreases to <2% between 37 and 222 mM H_2SO_4. This suggests that the detection method is accurate over a wide pH range if a higher d_1 is chosen to compensate for T_1 changes.

In Figure 3, even with a high recycle delay of 1.5 s, an unusually high error remains at the highest and lowest acid concentrations. The error at the lowest acid concentrations is in agreement with the results by Hodgetts et al. and is caused by deprotonation of MA below 20 mM H_2SO_4.[16] Spectra acquired at the highest acid concentration had phasing issues, which had to be corrected by postprocessing the spectrum using the autophasing algorithm in the software package MestReNova. We suspect that the phasing issues are caused by tuning and matching, which become more difficult at high salt concentrations.[14] To achieve maximum accuracy, the acid concentration should not exceed 222 mM.

As discussed previously, with the default settings of the ES pulse sequence, the acquisition time does not contribute to the percentage relaxation so that sensitivity is lost. To determine the maximum sensitivity for NH_4^+ detection with 1 mM Gd^{3+}, we deactivated the additional 90° pulse at the beginning of the pulse sequence so that both acquisition time and recycle delay contribute to the percentage relaxation. This leads to a significant increase in sensitivity (see Figure 4). The sensitivity can be further increased by reducing the interscan delay from $5T_1$ to $3T_1$ which is feasible in this case because the T_1 values of NH_4^+ and MA are very close to each other. The SNR of a 40 μM NH_4^+ sample measured for 14.6 min (interscan delay $3T_1$) is 47.4. This corresponds to a 1.4-fold sensitivity increase compared with the activated 90° pulse. The relative error is similar to an interscan delay of $5T_1$ and $3T_1$ (<6%), indicating that the interscan delay can be reduced without sacrificing accuracy. As discussed above, at high acid concentrations, a higher recycle than $3T_1$ might be necessary to compensate for T_1 changes.

We remeasured the sensitivity gain after addition of 1 mM Gd^{3+} to obtain a direct measurement of the sensitivity gain without the interference of the additional 90° pulse. Sensitivity increases of 3.9- and 3.6-fold are measured with 1 mM Gd^{3+} for interscan delays of $5T_1$ and $3T_1$, respectively. These values are consistent with the predicted sensitivity gain from the T_1

https://dx.doi.org/10.1021/acsomega.0c06130
ACS Omega 2021, 6, 5698−5704

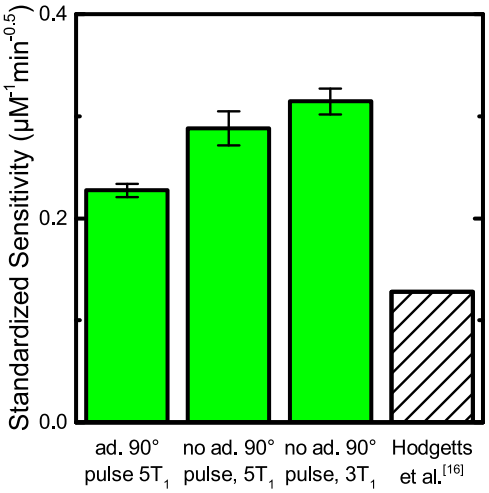

Figure 4. Effect on sensitivity of removing the additional 90° pulse from excitation sculpting pulse sequence and reducing the interscan delay from 0.72 s ($5T_1$) to 0.43 s ($3T_1$) (green). Comparison with literature sensitivity in water. A "standardized sensitivity" was calculated to compare sensitivities measured on different spectrometers (see main text). Error bars around each point represent the standard deviation for each triplicate measurement. NH_4^+: 40 μM, Gd^{3+}: 1 mM, field strength: 400 MHz.

decrease (3.9). Taking into account the corrected sensitivity gain that we calculated from Figure 1a (3.1), we estimate that the sensitivity can be increased by a factor of 3.5 ± 0.4 with 1 mM Gd^{3+}, which corresponds to an order of magnitude less analysis time or several hours less ammonia accumulation to reach the detection limit. This sensitivity improvement makes fast ^{1}H NMR NH_4^+ quantification accessible with a standard NMR spectrometer and reduces the cost of essential control experiments with expensive (≈500 euros/L) $^{15}N_2$.

It is difficult to compare the sensitivities of two different NMR detection methods if these methods were applied using different spectrometers. The sensitivity can vary an order of magnitude because of different field strength, probe hardware, NMR tubes, postprocessing methods, etc.[18] We attempt to compare our sensitivity with the sensitivity measured by Hodgetts et al. by calculating a standardized sensitivity that takes into account the influence of field strength and type of probe (cryo- or room-temperature probe) on sensitivity (Figure 4). The calculation of the standardized sensitivity can be found in the SI. As expected, with 1 mM Gd^{3+}, the standardized sensitivity is significantly higher than the value reported by Hodgetts et al. without Gd^{3+}.

CONCLUSIONS

In summary, the ^{1}H NMR analysis time required to quantify NH_4^+ in aqueous samples can be reduced by an order of magnitude by adding 1 mM paramagnetic Gd^{3+}. This improvement makes ^{1}H NMR NH_4^+ quantification more accessible and reduces the cost of control experiments with $^{15}N_2$, which enables faster, more reliable N_2 reduction research. A large reduction of the T_1 of NH_4^+ and MA without significant line broadening causes the sensitivity increase. The method has very good linearity (R^2 = 0.999) and is accurate over a wide pH range if the interscan delay is increased to compensate for small T_1 changes.

MATERIALS AND METHODS

Materials. $^{14}NH_4Cl$ (99.995%), $^{15}NH_4Cl$ (≥98 atom %, $^{15}N \geq 99$ % CP), maleic acid (≥99%), and H_2SO_4 (≥97.5%) were obtained from Sigma-Aldrich. Gadolinium(III) nitrate hexahydrate (99.9%) was obtained from Fisher Scientific. DMSO-d_6 (99.9% D, 0.03% V/V Tetramethylsilan) was obtained from Cambridge Isotope Laboratories. Ultrapure water was produced with a Milli-Q Advantage A10 water purification system (resistivity: 18.2 Ω at 25°C).

Sample Preparation. Ammonia standard solutions (40−500 μM) were prepared fresh daily by adding a suitable amount of NH_4Cl to ultrapure water and performing serial dilutions to the required standard concentrations. In a typical experiment, 525 μL of NH_4^+ standard solution was mixed with 50 μL of 0.5 M H_2SO_4, 50 μL of DMSO-d_6, 25 μL of 12.5 mM maleic acid, and 25 μL of 27 mM Gd^{3+} solution inside a 1.5 mL Eppendorf tube. This solution (600 μL) was transferred into a 5 mm thin-wall NMR tube (Wilmad). All NH_4^+ concentrations are reported as concentration in the NMR tube unless otherwise noted. The NMR tube was closed with Norell Sample Vault NMR tube caps (Sigma-Aldrich). The tube was cleaned with ultrapure water and ethanol using an NMR tube cleaner. After cleaning, the NMR tube was dried at 60°C for 1 h and stored in a dust-free environment.

^{1}H NMR Data Acquisition and Processing. ^{1}H NMR spectra were acquired on a 400 MHz pulsed Fourier transform NMR spectrometer equipped with an autosampler. An autotunable, temperature-regulated Agilent OneNMR room-temperature probe was used for all measurements. The temperature was set to 25 °C, and the receiver gain was optimized automatically. To avoid baseline distortions and low receiver gain, the water resonance has to be suppressed by a suitable pulse sequence. Good water suppression was obtained with pulse sequences that use pulsed field gradients to dephase the water magnetization and selective pulses to flip the NH_4^+ magnetization back into phase during acquisition. Two pulse sequences that were preinstalled in the software of our NMR system (vNMRj) were used in this work: Excitation Sculpting (vNMRj: "waterES") and double pulsed field gradient spin echo (vNMRj: "selexcit"). The waterES pulse sequence has the following structure:

waterES: G1-P90-G1-d1-P90-G2-S180-P180-G2-G3-S180-P180-G3-aq

where G1−G3 are the z-gradients of different strengths, P90 and P180 are hard pulses, and S180 is a selective 180° pulse. During the acquisition time, only the water resonance is out of phase, whereas the rest of the spectrum is in phase, leading to the desired suppression of the water resonance. The block "G1-P90-G1" dephases residual magnetization prior to the next scan and can be deactivated to increase sensitivity, as described in the main text. The z-gradient G1 had a duration of 1.6 ms and a strength of 1.07 G cm^{-1}. The z-gradients G2 and G3 had a duration of 1 ms and a strength of 1.7 G cm^{-1}. The 180° selective pulses had the shape "Wsupp" with a width of 2.5 ms and a power of 13 dB. The selexcit pulse sequence has the following structure:

selexcit: P90-G1-S180-G1-G2-S180-G2-aq

where G1 and G2 are the z-gradients of different strengths, P90 and P180 are hard pulses, and S180 is a selective 180° pulse. During the acquisition time, only the region defined by the selective 180° pulse is in phase, whereas the rest of the spectrum is out of phase. The z-gradients G1 and G2 had

https://dx.doi.org/10.1021/acsomega.0c06130
ACS Omega 2021, 6, 5698−5704

strengths of 0.85 and 1.28 G cm^{-1}, respectively, and a duration of 1 ms. The selective 180° pulse was defined as a "q3" pulse shape with a width of 5 ms and a power of 0 dB. The position and width of the selective pulse in the frequency domain were set to 6.63 ppm and 540 Hz, respectively, so that the pulse is positioned between the resonances of NH_4^+ and maleic acid. The pulse shapes q3 and "Wsupp" that were used to create the shaped pulses in waterES and selexcit are standard pulse shapes available in the software package vNMRj. Equivalent pulse shapes should be available in other software packages.

The data were processed in the software package MestReNova (version: 12.0.1-20560) using the automated tools provided in this software. Unless otherwise noted, an apodization of 4 Hz was applied followed by phasing and baseline correction. The peaks of NH_4^+ (*t*, ≈6.9 ppm, 4H) and MA (*s*, ≈6.21 ppm, 2H) were integrated using the line fitting tool. Using the line fitting tool instead of directly integrating the peaks leads to an approximately 2-fold decrease of the relative error. The three integrals of the NH_4^+ peaks were added together to calculate the total NH_4^+ integral. From the ratio of the integral of NH_4^+ and MA, the concentration of NH_4^+ was calculated with absolute quantification according to eq 2. The linewidth of NH_4^+ is calculated by averaging the full width at half-maximum (FWHM) of the three NH_4^+ peaks. The signal-to-noise ratio (SNR) was calculated using the "SNR calculation" tool in MestReNova with the noise region defined from 11 to 13 ppm. The SNR values were calculated by averaging three measurements of the average SNR of the three peaks of the NH_4^+ triplet. The relative error was calculated according to

$$\text{relative error} = \frac{c_{\text{calcd}} - c_{\text{grav}}}{c_{\text{grav}}} \times 100 \quad (5)$$

where c_{calcd} and c_{grav} are the concentrations of NH_4^+ calculated from absolute quantification and from the weight and purity of the NH_4Cl that was added to prepare the standards, respectively.

The T_1 values of NH_4^+ and MA were measured using the ES pulse sequence with default setting. Spectra were acquired at six different recycle delays, and the function $y(x) = a^*(1 - \exp(-bx))$ was fitted to the integrated peak intensities of NH_4^+ and MA as a function of d_1 using the software OriginPro 2015. Subsequently, the parameter b from the fitting function was inversed to calculate T_1. An example of the T_1 determination using this method can be found in the SI.

■ ASSOCIATED CONTENT

Supporting Information

The Supporting Information is available free of charge at https://pubs.acs.org/doi/10.1021/acsomega.0c06130.

Experimental details, calculations, and accuracy and linearity with $^{15}NH_4^+$ and T_1 determination (PDF)

■ AUTHOR INFORMATION

Corresponding Authors

Martin Kolen − *Materials for Energy Conversion and Storage (MECS), Department of Chemical Engineering, Delft University of Technology, 2629 HZ Delft, The Netherlands;* orcid.org/0000-0002-6309-4521; Email: m.kolen@tudelft.nl

Fokko M. Mulder − *Materials for Energy Conversion and Storage (MECS), Department of Chemical Engineering, Delft University of Technology, 2629 HZ Delft, The Netherlands;* orcid.org/0000-0003-0526-7081; Email: f.m.mulder@tudelft.nl

Author

Wilson A. Smith − *Materials for Energy Conversion and Storage (MECS), Department of Chemical Engineering, Delft University of Technology, 2629 HZ Delft, The Netherlands;* orcid.org/0000-0001-7757-5281

Complete contact information is available at: https://pubs.acs.org/10.1021/acsomega.0c06130

Notes

The authors declare no competing financial interest.

■ ACKNOWLEDGMENTS

This work is part of the Direct Electrolytic Ammonia Production project with project number 15234, which is financed by The Netherlands Organisation for Scientific Research (NWO). The authors thank Dr. Stephen Eustace and Zhiyu Liu for helpful discussions about paramagnetic relaxation agents.

■ REFERENCES

(1) Lan, R.; Irvine, J. T.; Tao, S. Ammonia and related chemicals as potential indirect hydrogen storage materials. *Int. J. Hydrogen Energy* **2012**, *37*, 1482−1494.

(2) Klerke, A.; Christensen, C. H.; Nørskov, J. K.; Vegge, T. Ammonia for hydrogen storage: challenges and opportunities. *J. Mater. Chem.* **2008**, *18*, 2304.

(3) Mulder, F. M. Implications of diurnal and seasonal variations in renewable energy generation for large scale energy storage. *J. Renewable Sustainable Energy* **2014**, *6*, No. 033105.

(4) MacFarlane, D. R.; Cherepanov, P. V.; Choi, J.; Suryanto, B. H.; Hodgetts, R. Y.; Bakker, J. M.; Ferrero Vallana, F. M.; Simonov, A. N. A Roadmap to the Ammonia Economy. *Joule* **2020**, *4*, 1186−1205.

(5) Andersen, S. Z.; et al. A rigorous electrochemical ammonia synthesis protocol with quantitative isotope measurements. *Nature* **2019**, *570*, 504−508.

(6) Yu, W.; Buabthong, P.; Read, C. G.; Dalleska, N. F.; Lewis, N. S.; Lewerenz, H.-J.; Gray, H. B.; Brinkert, K. Cathodic NH_4^+ leaching of nitrogen impurities in CoMo thin-film electrodes in aqueous acidic solutions. *Sustainable Energy Fuels* **2020**, *4*, 5080−5087.

(7) Choi, J.; Du, H.-L.; Nguyen, C. K.; Suryanto, B. H. R.; Simonov, A. N.; MacFarlane, D. R. Electroreduction of Nitrates, Nitrites, and Gaseous Nitrogen Oxides: A Potential Source of Ammonia in Dinitrogen Reduction Studies. *ACS Energy Lett.* **2020**, *5*, 2095−2097.

(8) Boucher, D. L.; Davies, J. A.; Edwards, J. G.; Mennad, A. An investigation of the putative photosynthesis of ammonia on iron-doped titania and other metal oxides. *J. Photochem. Photobiol., A* **1995**, *88*, 53−64.

(9) Krom, M. D. Spectrophotometric determination of ammonia: a study of a modified Berthelot reaction using salicylate and dichloroisocyanurate. *Analyst* **1980**, *105*, 305.

(10) *Nitrogen, Ammonia. Method 350.1 (Colorimetric, Automated, Phenate)*, revision 2.0; USEPA, 1993.

(11) Nielander, A. C.; et al. A Versatile Method for Ammonia Detection in a Range of Relevant Electrolytes via Direct Nuclear Magnetic Resonance Techniques. *ACS Catal.* **2019**, *9*, 5797−5802.

(12) Lin, Y.-X.; Zhang, S.-N.; Xue, Z.-H.; Zhang, J.-J.; Su, H.; Zhao, T.-J.; Zhai, G.-Y.; Li, X.-H.; Antonietti, M.; Chen, J.-S. Boosting selective nitrogen reduction to ammonia on electron-deficient copper nanoparticles. *Nat. Commun.* **2019**, *10*, No. 4380.

(13) Yu, W.; Lewis, N. S.; Gray, H. B.; Dalleska, N. F. Isotopically Selective Quantification by UPLC-MS of Aqueous Ammonia at

https://dx.doi.org/10.1021/acsomega.0c06130
ACS Omega 2021, 6, 5698−5704

Submicromolar Concentrations Using Dansyl Chloride Derivatization. *ACS Energy Lett.* **2020**, *5*, 1532−1536.
(14) Bharti, S. K.; Roy, R. Quantitative 1H NMR spectroscopy. *TrAC, Trends Anal. Chem.* **2012**, *35*, 5−26.
(15) Wider, G.; Dreier, L. Measuring Protein Concentrations by NMR Spectroscopy. *J. Am. Chem. Soc.* **2006**, *128*, 2571−2576.
(16) Hodgetts, R. Y.; Kiryutin, A. S.; Nichols, P.; Du, H.-L.; Bakker, J. M.; Macfarlane, D. R.; Simonov, A. N. Refining Universal Procedures for Ammonium Quantification via Rapid ^{1}H NMR Analysis for Dinitrogen Reduction Studies. *ACS Energy Lett.* **2020**, *5*, 736−741.
(17) Vosegaard, T.; Nielsen, N. C. Defining the sampling space in multidimensional NMR experiments: What should the maximum sampling time be? *J. Magn. Reson.* **2009**, *199*, 146−158.
(18) Ardenkjaer-Larsen, J.-H.; et al. Facing and Overcoming Sensitivity Challenges in Biomolecular NMR Spectroscopy. *Angew. Chem., Int. Ed.* **2015**, *54*, 9162−9185.
(19) Claridge, T. D. *High-Resolution NMR Techniques in Organic Chemistry*, 3th ed.; Elsevier: Oxford, United Kingdom, 2016; pp 469−475.
(20) Schanda, P.; Kupče, Ē.; Brutscher, B. SOFAST-HMQC Experiments for Recording Two-dimensional Deteronuclear Correlation Spectra of Proteins within a Few Seconds. *J. Biomol. NMR* **2005**, *33*, 199−211.
(21) Günther, H. *NMR Spectroscopy*, 3th ed.; Wiley-VCH: Weinheim, Germany, 2013; pp 239−247.
(22) Theillet, F.-X.; Binolfi, A.; Liokatis, S.; Verzini, S.; Selenko, P. Paramagnetic relaxation enhancement to improve sensitivity of fast NMR methods: application to intrinsically disordered proteins. *J. Biomol. NMR* **2011**, *51*, 487−495.
(23) Cai, S.; Seu, C.; Kovacs, Z.; Sherry, A. D.; Chen, Y. Sensitivity Enhancement of Multidimensional NMR Experiments by Paramagnetic Relaxation Effects. *J. Am. Chem. Soc.* **2006**, *128*, 13474−13478.
(24) Caravan, P.; Ellison, J. J.; McMurry, T. J.; Lauffer, R. B. Gadolinium(III) Chelates as MRI Contrast Agents: Structure, Dynamics, and Applications. *Chem. Rev.* **1999**, *99*, 2293−2352.
(25) Newman, J.; Thomas-Alyea, K. E. *Electrochemical Systems*, 3th ed.; Wiley-Interscience: Hoboken, NJ, 2004; pp 10−13.
(26) Burdyny, T.; Smith, W. A. CO_2 reduction on gas-diffusion electrodes and why catalytic performance must be assessed at commercially-relevant conditions. *Energy Environ. Sci.* **2019**, *12*, 1442−1453.

https://dx.doi.org/10.1021/acsomega.0c06130
ACS Omega 2021, 6, 5698−5704